

# Sulfide Controls on Mercury Speciation and Bioavailability to Methylating Bacteria in Sediment Pore Waters

JANINA M. BENOIT,\*<sup>†,‡</sup>  
 CYNTHIA C. GILMOUR,<sup>†</sup>  
 ROBERT P. MASON,<sup>‡</sup> AND  
 ANDREW HEYES<sup>†</sup>

*The Academy of Natural Sciences, Estuarine Research Center, 10545 Mackall Road, St. Leonard, Maryland 20685, and The University of Maryland, Center for Environmental and Estuarine Studies, Chesapeake Biological Laboratory, P.O. Box 38, Solomons, Maryland 20688*

A chemical equilibrium model for Hg complexation in sediments with sulfidic pore waters is presented. The purpose of the model was to explain observed relationships between pore water sulfide, dissolved inorganic Hg ( $Hg_D$ ), and bulk methylmercury (MeHg) in surficial sediments of two biogeochemically different ecosystems, the Florida Everglades and Patuxent River, MD. The model was constructed to test the hypothesis that the availability of Hg for methylation in sediments is a function of the concentration of neutral dissolved Hg complexes rather than  $Hg^{2+}$  or total  $Hg_D$ . The model included interaction of mercury with solids containing one or two sulfide groups, and it was able to reproduce observed  $Hg_D$  and bulk MeHg trends in the two ecosystems. The model is consistent with  $HgS^0$  as the dominant neutral Hg complex and the form of Hg accumulated by methylating bacteria in sulfidic pore waters. The model-estimated decline in  $HgS^0$  with increasing sulfide was consistent with the observed decline in bulk sediments MeHg. Since bacterial Hg uptake rate is one of the factors affecting methylation rate, Hg complexation models such as the one presented are helpful in understanding the factors that control MeHg production and accumulation in aquatic ecosystems.

## Introduction

We are interested in the chemical speciation of dissolved inorganic Hg ( $Hg_D$ ) in sediments pore waters because complexation of Hg may affect its bioavailability to the bacteria that produce methylmercury (MeHg). Sulfate-reducing bacteria (SRB) mediate methylation of inorganic Hg in aquatic sediments (1, 2), and these organisms produce sulfide as a byproduct of their metabolic activity. Methylation of Hg occurs inside SRB via enzyme-mediated transfer of a methyl group from B-12 (3, 4), but the Hg uptake mechanism in SRB is unknown. Sulfate both stimulates MeHg production and enhances the activity of SRB in sediments (2, 5), except under conditions where sulfide accumulation limits MeHg production (6–10). Sulfide inhibition has been ascribed to

the removal of Hg from solution via enhanced precipitation of  $HgS_{(s)}$  (7–9, 11) or to the formation of volatile dimethylmercury from reaction of MeHg with  $H_2S$  (6, 12).

Alternatively, we hypothesize that the availability of Hg for methylation is controlled by the concentration of neutral dissolved Hg complexes rather than  $Hg^{2+}$  or total  $Hg_D$ , because uptake occurs via passive diffusion across the cell membrane. The importance of neutral chloride species has previously been demonstrated for Hg uptake by phytoplankton (13, 14) and Hg permeability through artificial membranes (15). In sulfidic sediments, sulfide can out-compete other ligands for Hg complexation because of the extremely high formation constants of Hg–S complexes (e.g., refs 16 and 17). We suggest that  $HgS^0$  is the dominant neutral dissolved complex in sulfidic sediments and that the concentration of this complex affects microbial uptake and methylation. This hypothesis is consistent with the extremely low  $Hg^{2+}$  concentration in pore waters, and it describes a situation where dissolved complexes rather than free ions are most readily accumulated by microorganisms. Since MeHg production is a key step in Hg bioaccumulation, Hg complexation models are needed to predict methylation rates and to identify ecosystems vulnerable to accumulation of MeHg in food webs.

In this paper, we present a chemical equilibrium model for Hg speciation in sulfidic pore waters that can predict  $Hg_D$  measured in sediments from two very different ecosystems, the Florida Everglades and the Patuxent River Estuary. In both ecosystems, gradients in surface water sulfate lead to gradients in pore water sulfide as a result of bacterial sulfate reduction. However, the Patuxent is an estuarine system containing predominantly mineral sediments while the freshwater Everglades contain organic-rich peat. Our initial studies of Hg in these ecosystems (10, 18) indicated that MeHg production and accumulation in sediments is inversely correlated with pore water sulfide concentration in both systems. However,  $Hg_D$  is positively related to sulfide in the Patuxent while there is no relationship in the Everglades. This model is a first attempt at explaining both observed  $Hg_D$  and apparent bioavailability of Hg to methylating bacteria (as reflected by bulk MeHg concentration) in pore waters.

In developing the model, we first considered the simplest case (i.e., dissolution of excess cinnabar) to see how sensitive calculated  $Hg_D$  is to the choice of the intrinsic solubility and solubility product of cinnabar. Next, we modified the model to include sorption to solid phases in order to more adequately reflect observed trends in pore water  $Hg_D$ . The model was specifically designed to explain constant or increasing  $Hg_D$  with increasing sulfide concentration. Implicit in this model was the assumption that, in the presence of dissolved sulfide,  $HgS^0$  is the dominant form of Hg available for methylation; therefore, the trend in bulk sediments MeHg should reflect the concentration of this complex.

## Methods

**Field Sites.** Sampling and analysis of the two ecosystems modeled here are described in detail in Gilmour et al. (10) and Benoit et al. (18). In the Florida Everglades (USA), an extensive freshwater wetland, sediments were sampled from five sites over 80 km across a nutrient and sulfate gradient generated from agricultural runoff. The Patuxent River, a subestuary of the Chesapeake Bay with headwaters between Baltimore and Washington, DC, is impacted by urban and suburban development in its watershed. Samples were collected along a salinity gradient from the 60 km estuarine portion of this river.

\* Corresponding author e-mail: benoit@acnatsci.org; phone: (410)586-9700; fax: (410)586-9705.

<sup>†</sup> The Academy of Natural Sciences.

<sup>‡</sup> The University of Maryland.

**TABLE 1. Mercury–Sulfide Complexes and Equilibrium Constants ( $K_f$ ) Previously Reported in the Literature<sup>a</sup>**

reaction	$\log K_f$	reference
$\text{Hg}^{2+} + 2\text{HS}^- = \text{Hg}(\text{SH})_2^0$	37.7	16, 17, 28, 38, 41–43
$\text{Hg}^{2+} + 2\text{HS}^- = \text{HgS}_2\text{H}^- + \text{H}^+$	31.5	16, 17, 38, 41–43
$\text{Hg}^{2+} + 2\text{HS}^- = \text{HgS}_2^{2-} + 2\text{H}^+$	23.2	16, 17, 38, 41–43
$\text{Hg}^{2+} + \text{HS}^- = \text{HgSH}^+$	30.2	28, 41–43

<sup>a</sup>An average  $K_f$  from the literature is given where more than one reference was available.

**Sediment Sampling and Analysis.** The analysis presented here is based on surficial pore waters and bulk sediments (the top 0–4 cm). Sediment processing and analysis were the same in both ecosystems. Noncontaminating techniques (19, 20) were employed during all stages of sample collection, handling, and analysis. All cores were extruded and sectioned in an O<sub>2</sub>-free glovebox, and pore waters were separated via vacuum filtration through 0.2 μm (pore size) filters.

Sediment samples for total Hg (Hg<sub>T</sub>) were digested with a 5:2 mixture of HNO<sub>3</sub>:H<sub>2</sub>SO<sub>4</sub> prior to analysis. Pore waters were preserved with 1% HCl and digested with BrCl prior to analysis for Hg<sub>T</sub> by CVAFS (19, 21). MeHg analysis in both waters and sediments was carried out by distillation (22, 23), aqueous phase derivitization, and CVA detection (24). Typical detection limits and other quality control parameters for Hg and MeHg analysis in these sediments are given in Gilmour et al. (10) and Benoit et al. (18).

Subsamples of pore waters were preserved in sulfide antioxidant buffer (SAOB, 25). Sulfide was measured against a standard prepared in SAOB using an ion-specific electrode. The detection limit for sulfide analysis was about 0.1 μM.

**Modeling.** Equilibrium speciation calculations were carried out using the MINEQL<sup>+</sup> program (26). Average formation constants for Hg–S complexes that have been reported in the literature are given in Table 1. These values, rounded to the nearest 0.5 log unit, were used for the purposes of modeling. Choosing a value to use for the formation of HgS<sup>0</sup> is somewhat more problematic. A formation constant for this complex was not reported in the original determination of Schwarzenbach and Widmer (16). Its value can be calculated from the solubility product ( $K_{sp}$ ) of cinnabar (HgS(s) + H<sup>+</sup> = Hg<sup>2+</sup> + HS<sup>-</sup>) and the intrinsic solubility ( $K_{s1}$ ) of cinnabar (HgS(s) = HgS<sup>0</sup>), so that  $[\text{HgS}_{(\text{aq})}^0][\text{H}^+]/[\text{Hg}^{2+}][\text{HS}^-] = K_{s0} = K_{s1}/K_{sp}$ . The value of  $K_{s1}$  extrapolated from experimentally determined intrinsic solubilities of ZnS(s) and CdS(s) (17, 27, 28) combined with the solubility product for cinnabar originally determined by Schwarzenbach and Widmer (16) yields a estimate for  $\log K_{s0}$  of 26.7. The magnitude of  $\log K_{s0}$  was varied between 26 and 28 in the solubility model to illustrate how this constant affects model curves. A rounded value of 26.5 was used in the solid-phase model. A value of 10<sup>-17</sup> was used for the second dissociation constant of H<sub>2</sub>S as recommend by Dyrssen (27), and all other equilibrium constants were from the MINEQL<sup>+</sup> database.

The model solutions were in equilibrium with atmospheric CO<sub>2</sub> buffered with phosphate, and the pH was fixed at 7.0. Complexation was calculated across a 4 order of magnitude gradient in sulfide concentration (0.1 μM–1 mM). Ions included in the model were (total concentrations are given in parentheses) as follows: Na<sup>+</sup> (70 mM), K<sup>+</sup> (5mM), Mg<sup>2+</sup> (3 mM), Ca<sup>2+</sup> (1.5 mM), Fe<sup>2+</sup> (5 μM), Cl<sup>-</sup> (20 mM), PO<sub>4</sub><sup>3-</sup> (2 mM), and CO<sub>3</sub><sup>2-</sup> (50 mM). The only major ion that forms significant complexes with Hg is chloride, and varying the concentration of this ion across the entire salinity gradient in the Patuxent had no affect on the results of the model at the sulfide concentrations considered here.

The solubility product for HgS(s) represents an important input term; however, a range of values has been reported in

the literature over the past 30 years (see Table 2). To examine how  $K_{sp}$  affects Hg<sub>D</sub>, we considered a simple solubility model, the details of which are outlined in Table 3. Both of the simulations assume an excess of HgS(s). Simulations 1 and 2 address how the chosen values of  $K_{sp}$  and  $K_{s1}$ , respectively, affect Hg<sub>D</sub> in equilibrium with excess cinnabar.

To more adequately reflect processes occurring in aquatic sediments, a model that included interaction with solid phases was then formulated. In this model, HgS(s) did not precipitate as a pure solid. Instead this model was constructed to favor formation of solid-phase monosulfide or disulfide complexes via sorption of Hg. Details of this model are given in Table 4. The identity of “ROH” in reaction 6 is not specifically named; it may represent inorganic precipitates (e.g., iron oxyhydroxides) or organic particles. It is explicitly defined as a solid phase, so it is ascribed a concentration of unity in the model. Reaction 6 is a highly simplified representation of the early diagenetic formation of solids containing sulfide functional groups, such as FeS or organic thiols. The concentration of either of this type of solid should increase with increasing dissolved sulfide, as previous work has shown that sulfide produced from dissimilatory sulfate reduction is rapidly incorporated into both iron sulfides and organosulfides (29–32). The overall reactions for formation of solid-phase Hg complexes are given in reactions 9 and 10. The constants for these reactions include the unknown formation constants for RSH, so they cannot be estimated directly from known constants for binding of Hg(II) to thiols. The model was fit to the pore water and bulk MeHg data to derive  $K$  values for reactions 9 and 10.

Binding constants for Hg to thiol groups on DOC are similar in magnitude to Hg binding to bisulfide. In pore waters with very low sulfide and high DOC that is dominated by low molecular weight thiols, DOC complexation may play a role in solubilizing Hg. However, at the sulfide concentrations considered here, the concentration of thiol ligands on DOC will be very low as compared to the bisulfide. In the ecosystems modeled, the observed concentrations of Hg<sub>D</sub> can be adequately explained by in dissolved inorganic sulfide complexation alone.

## Results and Discussion

**Relationships between Sulfide, Hg<sub>D</sub>, and MeHg in Natural Sediments.** Dissolved inorganic mercury concentration versus dissolved sulfide is shown for sediments pore waters from two sites, the Patuxent River Estuary and the Florida Everglades in Figure 1. Hg<sub>D</sub> was calculated as the difference between pore water Hg<sub>T</sub> and MeHg. Both of these ecosystems exhibit a gradient in surface water sulfate that leads to a pore water sulfide gradient. However, the relationship between sulfide and Hg<sub>D</sub> differs between the two ecosystems. In the Everglades (Figure 1b), there is no significant relationship between the two parameters, whereas in the Patuxent (Figure 1a), Hg<sub>D</sub> increases with increasing sulfide ( $r^2 = 0.68$ ;  $P = 0.01$ ). The calculated partition coefficients ( $K_d = \text{ng of Hg (kg of sediment dw)}^{-1}/\text{ng of Hg (L of pore water)}^{-1}$ ) in the sediments at these two sites reflect the concentration trends (Figure 1, panels c and d). While  $K_d$  decreases with sulfide in the Patuxent, in the Everglades there is no significant change. The Everglades data in Figure 1 represent measurements from diverse sites sampled across several seasons, and Hg and sulfide analyses were performed on separate replicate cores at each site and date. Therefore, sampling variability, changes in the nature of the solid phases across the system, and non-sulfide ligands may contribute to the variability in the data.

In contrast, both sites show a decline in bulk sediments MeHg with sulfide (Figure 2). The Everglades trend is significant at  $P = 0.01$ ; the Patuxent trend is significant at  $P = 0.05$ . In the Everglades, in situ MeHg concentrations are

TABLE 2. Reported Values for  $K_{sp}$  of Cinnabar

	$\text{HgS(s)} = \text{Hg}^{2+} + \text{S}^{2-}$	$\log K_1$	
	$\text{H}^+ + \text{S}^{2-} = \text{HS}^-$	$\log K_2$	
	$\text{HgS(s)} + \text{H}^+ = \text{Hg}^{2+} + \text{HS}^-$	$\log K_{sp} = \log K_1 + \log K_2$	
source		$\log K_1$	$\log K_2$
Schwarzenbach and Widmer (16)		-50.9	14.2
Dyrssen (27)		-55.5	17.0
Paquette and Helz (38)		-53.7	17.0
Dyrssen (41)		-51.0	14.1
Smith and Martell (44)		-52.7	13.9
Stumm and Morgan (45)		-52.7	13.9
Dyrssen and Kremling (46)		-55.9	17.0
		$\log K_{sp}$	
		-36.7	
		-38.5	
		-36.7	
		-36.9	
		-38.8	
		-38.8	
		-38.9	

TABLE 3. Mercury-Sulfide Complexes and Equilibrium Constants ( $K_f$ ) Used in the Speciation Models for Dissolved Hg in the Presence of Excess Cinnabar

complex	$\log K_f$
$\text{Hg}^{2+} + 2\text{HS}^- = \text{Hg}(\text{SH})_2^0$	37.5
$\text{Hg}^{2+} + 2\text{HS}^- = \text{HgS}_2\text{H}^- + \text{H}^+$	32.0
$\text{Hg}^{2+} + 2\text{HS}^- = \text{HgS}_2^{2-} + 2\text{H}^+$	23.5
$\text{Hg}^{2+} + \text{HS}^- = \text{HgSH}^+$	30.5
simulation 1	
$\text{HgS(s)} + \text{H}^+ = \text{Hg}^{2+} + \text{HS}^-$	$\log K_{sp} = -38, -37, -36$
$\text{HgS(s)} = \text{HgS}^0$	$\log K_{s1} = -10$
$\text{Hg}^{2+} + \text{HS}^- = \text{HgS}^0 + \text{H}^+$	$\log K_{s0} = -28, -27, -26$
simulation 2	
$\text{HgS(s)} + \text{H}^+ = \text{Hg}^{2+} + \text{HS}^-$	$\log K_{sp} = -37$
$\text{HgS(s)} = \text{HgS}^0$	$\log K_{s1} = -11, -10, -9$
$\text{Hg}^{2+} + \text{HS}^- = \text{HgS}^0 + \text{H}^+$	$\log K_{s0} = -28, -27, -26$

TABLE 4. Mercury-Sulfide Complexes and Equilibrium Constants ( $K_f$ ) Used in the Speciation Models for Dissolved Hg with Sorption to the Solid Phase

dissolved species	$\log K_f$	
$\text{Hg}^{2+} + 2\text{HS}^- = \text{Hg}(\text{SH})_2^0$	37.5	(1)
$\text{Hg}^{2+} + 2\text{HS}^- = \text{HgS}_2\text{H}^- + \text{H}^+$	32.0	(2)
$\text{Hg}^{2+} + 2\text{HS}^- = \text{HgS}_2^{2-} + 2\text{H}^+$	23.5	(3)
$\text{Hg}^{2+} + \text{HS}^- = \text{HgSH}^+$	30.5	(4)
$\text{Hg}^{2+} + \text{HS}^- = \text{HgS}^0 + \text{H}^+$	26.5	(5)
solid species	reaction type	
$\text{ROH} + \text{HS}^- = \text{RSH} + \text{OH}^-$	solid-phase thiol formation	(6)
$\text{RSH} + \text{Hg}^{2+} = \text{RSHg}^+ + \text{H}^+$	sorption to solid	(7)
$2\text{RSH} + \text{Hg}^{2+} = (\text{RS})_2\text{Hg} + 2\text{H}^+$	sorption to solid	(8)
net reactions	$\log K_f$	
$\text{ROH} + \text{HS}^- + \text{Hg}^{2+} = \text{RSHg}^+ + \text{H}_2\text{O}$	unknown	(9)
$2\text{ROH} + 2\text{HS}^- + \text{Hg}^{2+} = (\text{RS})_2\text{Hg} + 2\text{H}_2\text{O}$	unknown	(10)

well correlated with methylation rates (10) measured using a radio tracer (33). This suggests that concentration serves as a surrogate for production in ecosystems without significant exogenous sources of MeHg. Thus, we propose that the decrease in MeHg across the sulfide gradient reflects the decreased availability of  $\text{Hg}_D$ . As indicated above, passive uptake via diffusion depends on the concentration of neutral

species, and the mechanism of sulfide inhibition of Hg methylation may be a shift in speciation away from a dominant neutral complex at higher sulfide concentrations.

**Cinnabar Solubility Model.** Predicted  $\text{Hg}_D$  curves generated by the pure cinnabar solubility model (Figure 3) indicate that in the presence of excess  $\text{HgS(s)}$  dissolved Hg increases with increasing sulfide concentration (except at unrealistically low values of  $K_{sp}$ ). As indicated in Figure 3a, the value of  $K_{sp}$  determines the maximum  $\text{Hg}_D$  present at high sulfide. The minimum  $\text{Hg}_D$  at low sulfide is determined by the chosen value of  $K_{s1}$ , as illustrated by Figure 3b. The value for  $K_{s1}$  that has been proposed by Dyrssen and Wedborg (17, 27, 28),  $10^{-10}$  M, is more than 1 order of magnitude above the  $\text{Hg}_D$  observed at low sulfide in the Everglades and Patuxent River sediments.

The concentration of the various Hg-sulfide species for the solubility model is shown for  $\log K_{sp} = -37$ ,  $K_{s1} = 10^{-10}$  M in Figure 4. Notice that the concentration of  $\text{HgS}^0$  is constant across the sulfide gradient, but that  $\text{Hg}(\text{HS})_2^0$  increases until it becomes the dominant neutral complex at high sulfide. As a result, the total concentration of neutral species does not decrease with increasing sulfide with this model.

**Solid-Phase Model.** A model that attempts to explain observed  $\text{Hg}_D$  and bulk MeHg trends in these sediments pore waters must reconcile the following points: (i)  $\text{Hg}_D$  is always below the intrinsic solubility of cinnabar, (ii)  $\text{Hg}_D$  may be constant with increasing sulfide concentration, and (iii) the bioavailability of Hg (as indicated by methylation) decreases with increasing sulfide, which suggests that the concentration of neutral species also decreases.

The failure of a pure-phase solubility model to estimate realistic concentrations of  $\text{Hg}_D$ , its inability to explain the constant  $\text{Hg}_D$  of the Everglades, and its prediction of constant  $\text{HgS}^0$  makes it unsatisfactory for describing in situ controls on pore water Hg and bulk sediments MeHg in these ecosystems. An alternative model that includes adsorption to (or coprecipitation with) the solid phase was formulated to determine if the above criteria could be met (Table 4). In this solid-phase model, cinnabar does not form as a pure phase because of the excess of sorbing solids, and the reaction for  $\text{HgS(s)}$  formation was not included. The existence of pure  $\text{HgS(s)}$  in sediments is doubtful given the propensity of Hg to be incorporated into Fe-sulfide (34) or organic (35, 36) solid phases. The model present here does not distinguish between inorganic or organic solid sulfides. A total Hg concentration of 50 nM was used. Since the reaction for the formation of the thiol "RSH" was combined into the reactions for the formation of  $\text{RSHg}^+$  and  $(\text{RS})_2\text{Hg}$ , the only variables in the model are the formation constants for these two mixed solids. In this formulation, the  $K$  values for the solid-phase reactions are influenced by a number of factors including the size, shape, and charge distribution at the surface of the

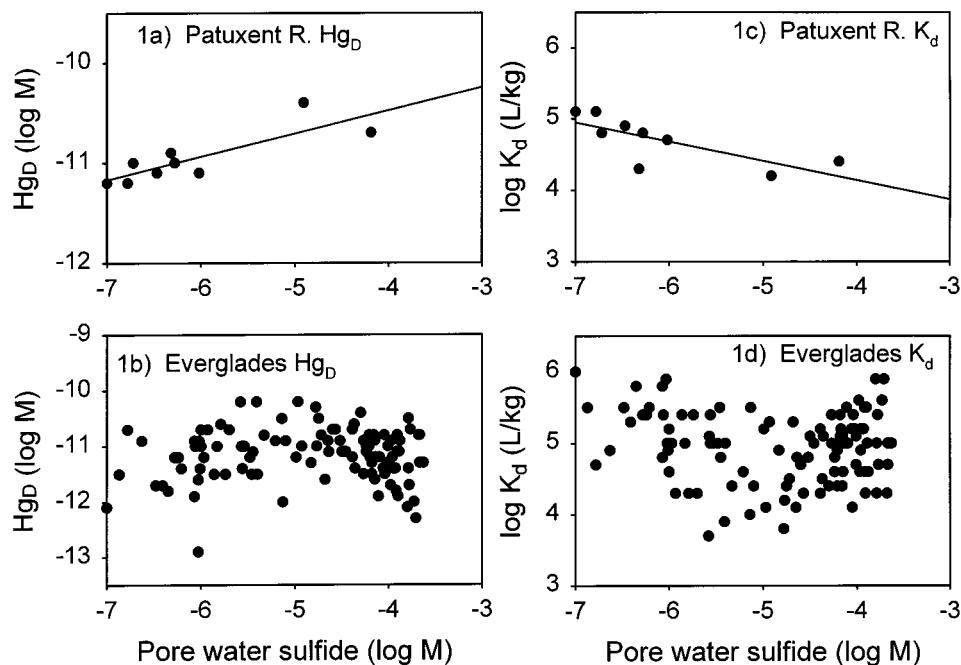


FIGURE 1. Dissolved inorganic Hg concentration and  $\log K_d$  versus sulfide concentration in pore waters from surficial sediments (0–4 cm) from (a and c) the Patuxent River Estuary (September 1995) and (b and d) the Florida Everglades (June 1995–1997).

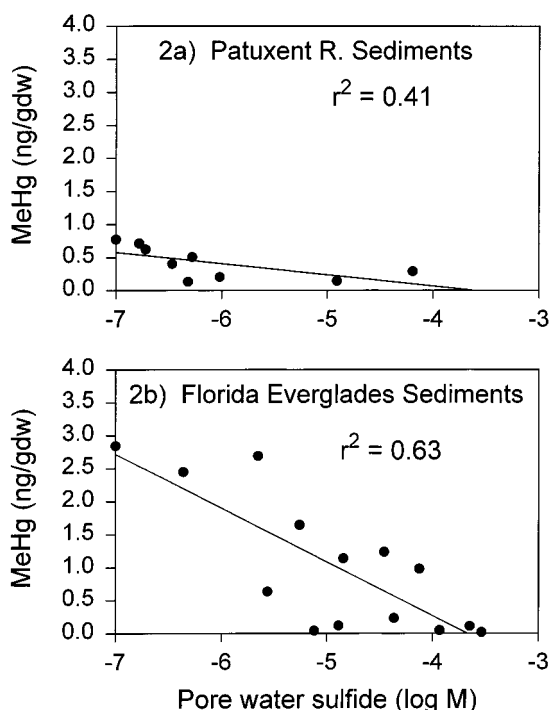


FIGURE 2. Methylmercury concentration in bulk sediments versus pore water sulfide concentration in surficial sediments (0–4 cm) from (a) the Patuxent River Estuary (September 1995) and (b) the Florida Everglades (June 1995–1997).

model thiol. As such, they are effective equilibrium constants, and they are expected to vary somewhat across ecosystems due to the nature of sedimentary particles.

The concentrations of  $\text{HgS}^0$  and  $\text{HgHS}_2^-$  across a sulfide gradient were calculated using the solid-phase model (Figure 5). In the model, all of the dissolved Hg was present as sulfide complexes, and these are the two major complexes. The concentration of  $\text{Hg}^{2+}$  was about 30 orders of magnitude lower than any Hg–S complex across the gradient. Figure 5a shows that, over the range of  $\log K$  for  $\text{RSHg}^+$  examined, the

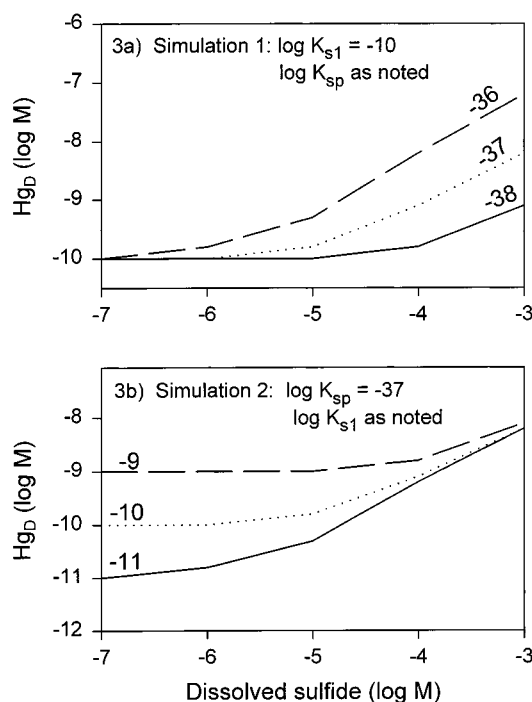


FIGURE 3. Dissolved inorganic Hg as a function of sulfide concentration calculated using the solubility model (excess cinnabar present). For details see Table 3.

concentration of  $\text{HgS}^0$  always decreases with increasing sulfide. However, as the value of  $K$  increases, the concentration of  $\text{HgS}^0$  becomes constant at lower sulfide concentrations. At high  $K$  for  $\text{RSHg}^+$ , virtually all of the Hg is bound to this solid, the concentration of  $\text{RSHg}^+$  is constant, and the concentration of  $\text{HgS}^0$  is buffered by the reaction:  $\text{RSHg}^+ + \text{H}_2\text{O} = \text{ROH} + \text{HgS}^0 + \text{H}^+$ . The buffered concentration of  $\text{HgS}^0$  is determined by (i) the difference between  $\log K$  values for  $\text{RSHg}^+$  and  $\text{HgS}^0$  and (ii) the total Hg concentration. On the other hand, the concentration of  $\text{HgHS}_2^-$  becomes fixed when the  $K$  for  $\text{RSHg}^+$  is low relative to  $(\text{RS})_2\text{Hg}$  (Figure 5b)

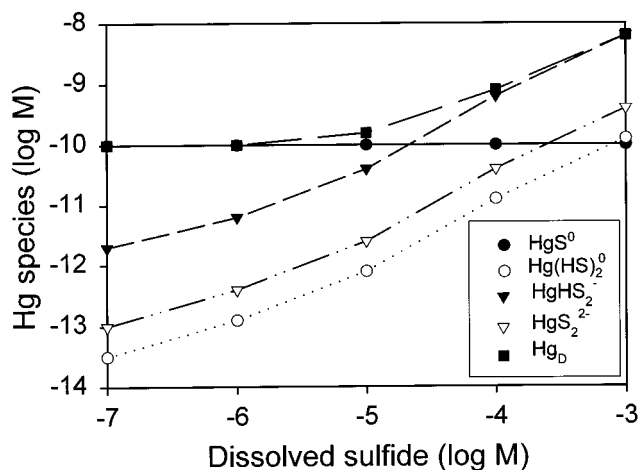


FIGURE 4. Hg speciation as a function of sulfide concentration calculated using the solubility model with  $K_{sp} = -37$  and  $K_{s1} = -10$ . Constants for other complexes as in Table 3.

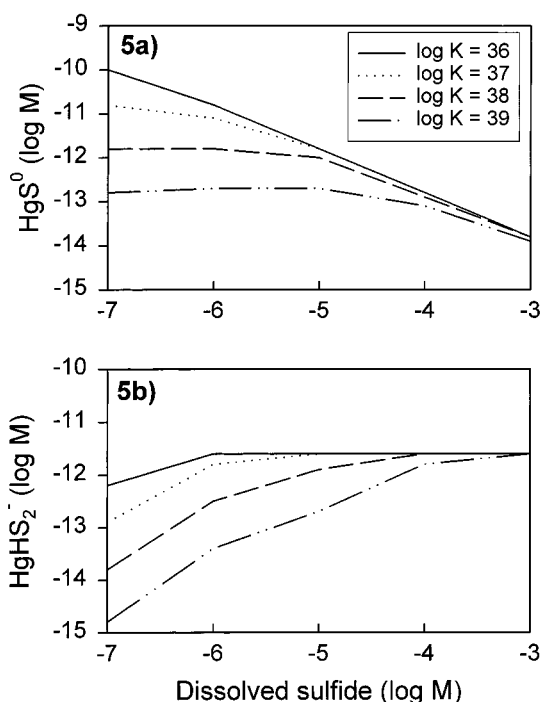


FIGURE 5. Changes in the concentration of (a)  $\text{HgS}^0$  and (b)  $\text{HgHS}_2^-$  as a function of sulfide concentration calculated using the solid-phase model. The  $\log K$  for formation of  $\text{HgSR}^+$  was varied as noted; the value of  $\log K$  for  $\text{Hg}(\text{SR})_2$  was set at 43.

because of a similar buffering mechanism by the reaction:  $(\text{RS})_2\text{Hg} + 2\text{H}_2\text{O} = 2\text{ROH} + \text{HgHS}_2^- + \text{H}^+$ .

At high  $K$  for  $\text{RSHg}^+$  relative to  $(\text{RS})_2\text{Hg}$ , the concentration of  $\text{HgHS}_2^-$  and all the other disulfide species including  $(\text{RS})_2\text{Hg}$  increase with increasing sulfide (Figure 5b). It is important to note that, because  $\text{RSHg}^+$  and  $(\text{RS})_2\text{Hg}$  are not pure solids, they are allowed to have varying activities (i.e., they are treated as complexes) rather than having a constant activity of 1 once formed. This allows for changing concentrations of  $\text{HgS}^0$  and  $\text{HgHS}_2^-$  at intermediate values of  $K$ , where both solids are sorbing some of the available Hg.

The formation of a singly or doubly coordinated surface complex results in  $\text{Hg}_D$  that can increase, remain constant, or decrease as a function of sulfide concentration (Figure 6a). The concentration of  $\text{HgS}^0$  exceeds  $\text{HgHS}_2^-$  at low sulfide; at higher sulfide  $\text{HgHS}_2^-$  is the dominant complex determining  $\text{Hg}_D$  (see Figure 5). Therefore, the  $\text{Hg}_D$  model curves

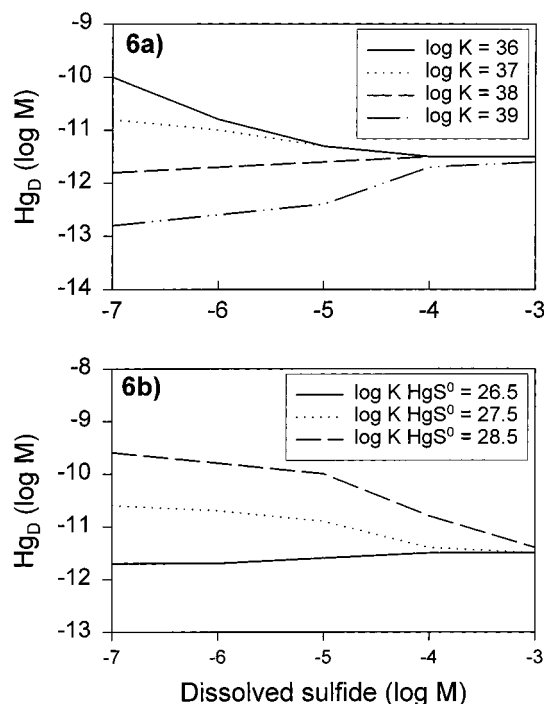


FIGURE 6. Dissolved inorganic Hg as a function of sulfide concentration calculated using the solid-phase model: (a)  $\log K$  for formation of  $\text{HgSR}^+$  was varied as noted, and  $\log K$  for  $\text{Hg}(\text{SR})_2$  was set at 43; (b)  $\log K$  for formation of  $\text{HgSR}^+$  was set at 38,  $\log K$  for  $\text{Hg}(\text{SR})_2$  was set at 43, and  $\log K_{s0}$  for  $\text{HgS}^0$  was varied as noted.

depend not only of the magnitudes of  $K$  for  $\text{RSHg}^+$  and  $(\text{RS})_2\text{Hg}$  relative to one another but also on the magnitude of the  $K$  for  $\text{RSHg}^+$  relative to  $\text{HgS}^0$ . As illustrated in Figure 6b, values of  $K_{\text{RSHg}^+}$  and  $K_{(\text{RS})_2\text{Hg}}$  which produce slightly increasing  $\text{Hg}_D$  with a  $\log K_{s0}$  of 26.5, yield decreasing  $\text{Hg}_D$  as  $\log K_{s0}$  is increased. For modeling the field data, we used a value of 26.5 for the formation of  $\text{HgS}^0$ , and only the values of  $K$  for  $\text{RSHg}^+$  and  $(\text{RS})_2\text{Hg}$  were varied.

**Model Fit to Field Data.** The solid-phase model was fit to the  $\text{Hg}_D$  data for the Patuxent River (Figure 7a) and the Everglades (Figure 7b). The "total Hg" values for MINEQL<sup>+</sup> were estimated as the average Hg concentration ( $\text{ng g}^{-1}$  wet weight) divided by the average water content ((g of water)  $\text{g}^{-1}$  wet weight) for surface sediments at each site. This allowed the Hg content of the whole sediments to be expressed on a molar basis. The calculated Hg concentrations were  $0.05 \pm 0.03 \mu\text{M}$  for the Everglades and  $0.2 \pm 0.03 \mu\text{M}$  for the Patuxent River. The constants for the two solids that best predicted observed  $\text{Hg}_D$  were similar between the two sites:  $\log K_{\text{RSHg}^+} = 38$ ,  $\log K_{(\text{RS})_2\text{Hg}} = 42$  for the Patuxent, and  $\log K_{\text{RSHg}^+} = 37.5$ ,  $\log K_{(\text{RS})_2\text{Hg}} = 42.5$  for the Everglades. Somewhat different ligand strengths in these ecosystems are not surprising because of the nature of the solid-phase matrix in each; in the Patuxent it is primarily mineral, in the Everglades it is primarily organic.

In addition to being able to reproduce the observed  $\text{Hg}_D$  distributions in the two ecosystems (Figure 7, panels a and b), the solid-phase model predicts a decrease in the concentration of neutral Hg species with increasing sulfide for both sites. The model-generated concentration of dissolved neutral Hg complexes (predominantly  $\text{HgS}^0$ ) is plotted against bulk MeHg in Figure 7, panels c and d. In both ecosystems, about 50% of the trend in the MeHg concentration can be accounted for by this variable. This relationship adds credence to the hypothesis that neutral complexes exert an important control on the availability of Hg for methylation. The amount of MeHg produced in sediments depends on a

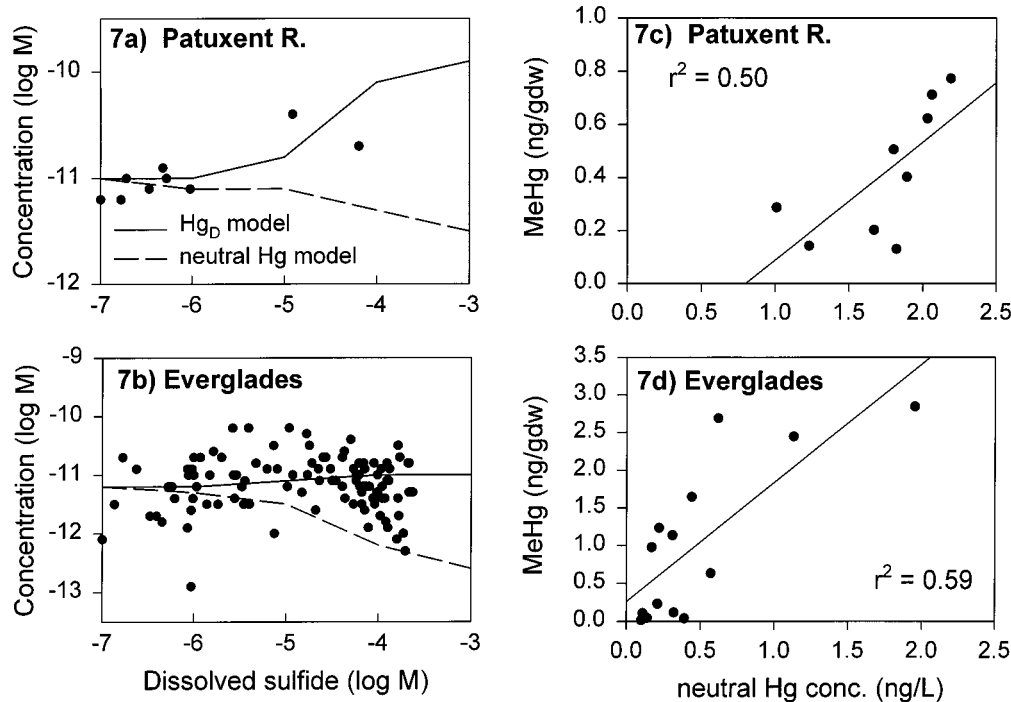


FIGURE 7. Solid-phase model fit to Hg data from surficial sediments pore waters in the (a) the Everglades and (b) the Patuxent River Estuary. The predicted concentration of neutral Hg species ( $\text{HgS}^0 + \text{Hg}(\text{HS})_2^0$ ) and dissolved inorganic Hg are shown as lines; data are shown as points. The concentrations of bulk MeHg and dissolved neutral Hg concentration in pore waters are compared for the (c) Everglades and (d) the Patuxent River Estuary.

number of parameters including pH, temperature, and organic matter content (9, 37) in addition to the concentration of available Hg. The steeper slope in Figure 7d suggests that a larger fraction of available  $\text{Hg}_D$  is converted to MeHg in the Everglades, which may be due to higher temperatures and greater supplies of labile organic matter.

**Potentially Important Solid Phases.** The current model can include metal sulfides in addition to or in place of organic thiols as the important solid-phase ligands for Hg. Thus, the solid-phase interactions could represent coprecipitation with metal monosulfides or the pyritization of Hg. The model reactions can be rewritten to include formation of metal sulfides ( $\text{X}^{2+} + \text{HS}^- = \text{XS} + \text{H}^+$  and  $\text{XS} + \text{HS}^- = \text{XS}_2 + \text{H}^+ + 2\text{e}^-$ ) and replacement by Hg ( $\text{XS} + \text{Hg}^{2+} = \text{HgS} + \text{X}^{2+}$  and  $\text{XS}_2 + \text{Hg}^{2+} = \text{HgS}_2 + \text{X}^{2+}$ ). The net reactions are equivalent to those used in the "thiol" model as long as  $\text{X}^{2+}$  is present in large excess of  $\text{Hg}^{2+}$ . In all but highly Hg contaminated sediments, the concentrations of other metals (especially  $\text{Fe}^{2+}$ ) are orders of magnitude higher than  $\text{Hg}^{2+}$ , so the assumption will generally be met. As defined here, HgS and  $\text{HgS}_2$  are not pure solids because they exist within a matrix of iron monosulfide and pyrite, so they are analogous to  $\text{RSHg}^+$  and  $(\text{RS})_2\text{Hg}$ .

**Significance of the Solid-Phase Model.** Results of chemical equilibrium modeling efforts presented here suggest that cinnabar precipitation and dissolution as a pure phase may not be the important processes controlling  $\text{Hg}_D$  in sulfidic pore waters. A simple solubility model estimates sharply increasing  $\text{Hg}_D$  with increasing sulfide, while field observations are of constant or modestly increasing  $\text{Hg}_D$  in surficial pore waters from the Everglades and the Patuxent River. Furthermore, the presence of pure cinnabar in these sediments would lead to a constant  $\text{HgS}^0$  across the sulfide gradient, which is at odds with the observed decline in MeHg with increasing sulfide, assuming that this complex controls bioavailability to methylating bacteria. Some past models have not included  $\text{HgS}^0$  in explaining Hg solubility (38, 39); however, our model results and the observed MeHg distri-

butions suggest that  $\text{HgS}^0$  is the major neutral complex in sulfidic sediments. Measurement of octanol-water partitioning of Hg across a sulfide gradient (40) indicated a  $K_{ow}$  for  $\text{HgS}^0$  of about 25, with a strong decrease in the hydrophobicity of Hg as the concentration of this complex decreased, which further supports the model presented here.

The important features of our alternative model include the following: (i) formation of solid thiols, which depends on sulfide concentration; (ii) sorption of Hg to these solids with coordination to one or two surface sulfide groups; and (iii) resultant Hg-associated solids that are not pure phases. This model is a simplification of a number of complex reactions, and it is intended to serve as a starting point for identifying some of the processes that control Hg dynamics in reduced sediments.

While this is not the only model that can explain the data sets presented, it successfully reproduces dissolved Hg concentrations that are similar in magnitude and trend to those in pore waters from two ecosystems. This model predicts either constant or increasing  $\text{Hg}_D$ , as well as decreasing  $\text{HgS}^0$  with increasing sulfide, with the magnitude of the  $\text{Hg}_D$  change driven by the relative strength of the binding of Hg to the two solid phases. It remains to be determined if sorption to organic thiols, coprecipitation with metal sulfides, or other processes are in fact important in controlling Hg solubility and speciation in aquatic sediments. Work by Huerta-Diaz and Morse (34) has shown a high degree of pyritization for Hg relative to other trace metals in anoxic marine sediments. On the other hand, Hg was found to be predominantly associated with organic solids in Saguenay Fjord sediments (35) and lake sediments from a hydroelectric reservoir (36). Determination of Hg-solid associations using sequential leaching and other techniques are needed to further elucidate the solid-phase complexation of Hg in the Everglades and the Patuxent River Estuary.

The model generates concentration trends in  $\text{HgS}^0$  that are consistent with MeHg distribution observed in these two ecosystems. The model-estimated decline in  $\text{HgS}^0$  with sulfide

agrees not only in sense but also in magnitude with measured MeHg concentrations. This close correspondence supports the hypothesis that Hg<sup>0</sup> is the form of Hg accumulated by methylating bacteria in sulfidic sediments. The model is consistent with passive uptake limiting biotic Hg methylation and may explain the inverse relationship between sulfide and MeHg seen across sulfate and salinity gradients in estuarine (6–8) and freshwater sediments (9, 10). Therefore, it may be useful in developing future models for a priori prediction of MeHg production and accumulation in aquatic ecosystems.

### Acknowledgments

Work in Florida was supported by EPA/ORD Assistance Agreement CR823735, South Florida Water Management District (SFWMD) Contract C-7690, and Florida DEP Contract SP-434. Field support was provided by both the SFWMD and the USGS South Florida Ecosystem Program. Work in Maryland was supported by Maryland DNR through the Power Plant Topical Research Program, Grant CB95-004=002. J.M.B. was supported by a Chesapeake Biological Laboratory Fellowship and an EPA Star Fellowship. We thank G. S. Riedel, J. T. Bell, and M. E. Hagy for technical and field assistance.

### Literature Cited

- (1) Compeau, G.; Bartha, R. *Appl. Environ. Microbiol.* **1985**, *50*, 498.
- (2) Gilmour, C. C.; Henry, E. A.; Mitchell, R. *Environ. Sci. Technol.* **1992**, *26*, 2281.
- (3) Choi, S.-C.; Bartha, R. *Appl. Environ. Microbiol.* **1993**, *59*, 290.
- (4) Choi, S.-C.; Chase, T., Jr.; Bartha, R. *Appl. Environ. Microbiol.* **1994**, *60*, 1342.
- (5) Krabbenhoft, D. P.; Gilmour, C. C.; Benoit, J. M.; Babiarz, C. L.; Andren, A. W.; Hurley, J. P. *Can. J. Fish. Aquat. Sci.* **1998**, *55*, 835.
- (6) Craig, P. J.; Moreton, P. A. *Mar. Pollut. Bull.* **1983**, *14*, 408.
- (7) Compeau, G.; Bartha, R. *Bull. Environ. Contam. Toxicol.* **1983**, *31*, 486.
- (8) Compeau, G.; Bartha, R. *Appl. Environ. Microbiol.* **1987**, *53*, 261.
- (9) Winfrey, M. R.; Rudd, J. W. M. *Environ. Toxicol. Chem.* **1990**, *9*, 853.
- (10) Gilmour, C. C.; Riedel, G. S.; Ederington, M. C.; Bell, J. T.; Benoit, J. M.; Gill, G. A.; Stordal, M. C. *Biogeochemistry* **1998**, *80*, 327.
- (11) Blum, J. E.; Bartha, R. *Contam. Toxicol.* **1980**, *25*, 404.
- (12) Craig, P. J.; Bartlett, P. D. *Nature* **1978**, *275*, 635.
- (13) Mason, R. P.; Reinfelder, J. R.; Morel, F. M. M. *Environ. Sci. Technol.* **1996**, *30*, 1835.
- (14) Mason, R. P.; Reinfelder, J. R.; Morel, F. M. M. *Water Air Soil Pollut.* **1995**, *80*, 915.
- (15) Gutknecht, J. J. *J. Membr. Biol.* **1981**, *61*, 61.
- (16) Schwarzenbach, G.; Widmer, M. *Helv. Chim. Acta* **1963**, *46*, 2613.
- (17) Dyrssen, D.; Wedborg, M. *Water Air Soil Pollut.* **1991**, *56*, 507.
- (18) Benoit, J.; Gilmour, C. C.; Mason, R. P.; Riedel, G. F.; Riedel, G. S. *Biogeochemistry* **1998**, *80*, 249.
- (19) Gill, G. A.; Fitzgerald, W. F. *Mar. Chem.* **1987**, *20*, 227.
- (20) Flegal, A. R.; Smith, G. J.; Gill, G. A.; Sanudo-Wilhelmy, S.; Anderson, L. C. D. *Mar. Chem.* **1991**, *36*, 329.
- (21) Bloom, N.; Fitzgerald, W. F. *Anal. Chim. Acta* **1988**, *208*, 151.
- (22) Horvat, M.; Bloom, N. S.; Liang, L. *Anal. Chim. Acta* **1993**, *282*, 135.
- (23) Horvat, M.; Liang, L.; Bloom, N. S. *Anal. Chim. Acta* **1993**, *282*, 153.
- (24) Bloom, N. *Can. J. Fish. Aquat. Sci.* **1989**, *46*, 1131.
- (25) Brouwer, H.; Murphy, T. P. *Environ. Toxicol. Chem.* **1994**, *13*, 1273.
- (26) Schecker, W. D.; McAvoy, D. C. *MINEQL+ Version 2.1: A chemical equilibrium program for personal computer*, The Proctor and Gamble Co.: Cincinnati, OH, 1991.
- (27) Dyrssen, D. *Mar. Chem.* **1989**, *28*, 241.
- (28) Dyrssen, D.; Wedborg, M. *Mar. Chem.* **1989**, *26*, 289.
- (29) David, M. B.; Mitchell, M. J. *Limnol. Oceanogr.* **1985**, *30*, 1196.
- (30) Rudd, J. W. M.; Kelly, C. A.; Furutani, A. *Limnol. Oceanogr.* **1986**, *31*, 1281.
- (31) Brüchert, V.; Pratt, L. M. *Geochim. Cosmochim. Acta* **1996**, *13*, 2325.
- (32) Canfield, D. E.; Boudreau, D. P.; Mucci, A.; Gundersen, J. K. *Geochim. Cosmochim. Acta* **1996**, *13*, 2325.
- (33) Gilmour, C. C.; Riedel, G. S. *Water Air Soil Pollut.* **1995**, *80*, 747.
- (34) Huerta-Diaz, M. A.; Morse, J. W. *Geochim. Cosmochim. Acta* **1992**, *56*, 2681.
- (35) Bono, A. B. M.S. Dissertation, McGill University, Montreal, 1997.
- (36) Dmytriw, R.; Mucci, A.; Lucotte, M.; Pichet, P. *Water Air Soil Pollut.* **1995**, *80*, 1099.
- (37) Gilmour, C. C.; Henry, E. A. *Environ. Pollut.* **1991**, *71*, 131.
- (38) Paquette, K.; Helz, G. *Water Air Soil Pollut.* **1995**, *80*, 1053.
- (39) Paquette, K.; Helz, G. *Environ. Sci. Technol.* **1997**, *31*, 2148.
- (40) Benoit, J. M.; Mason, R. P.; Gilmour, C. C. Submitted to *Environ. Toxicol. Chem.*
- (41) Dyrssen, D. *Mar. Chem.* **1988**, *24*, 143.
- (42) Henry, E. A. Dissertation, Harvard University, Cambridge, 1992.
- (43) Paquette, K. Ph.D. Dissertation, University of Maryland, College Park, 1994.
- (44) Smith, R. M.; Martell, P. E. *Critical Stability Constants, Vol. 4, Inorganic Complexes*; Plenum: New York, 1976.
- (45) Stumm, W.; Morgan, J. J. *Aquatic Chemistry*; John Wiley and Sons: New York, 1981.
- (46) Dyrssen, D.; Kremling, K. *Mar. Chem.* **1990**, *30*, 193.

Received for review August 12, 1998. Revised manuscript received December 14, 1998. Accepted December 22, 1998.

ES9808200